The 2009 IEEE/RSJ International Conference on
Intelligent Robots and Systems
October 11-15, 2009 St. Louis, USA

# 3D Limit Cycle Walking of Musculoskeletal Humanoid Robot with Flat Feet

Kenichi Narioka, Shinpei Tsugawa, and Koh Hosoda

*Abstract*— **Most of traditional biped walkers based on passive dynamic walking have arc feet and locked ankle joints. In this paper, we propose the method to substitute the arc feet with flat feet. We hypothesize that the shape of the arc feet corresponds to a circular roll-over shape (ROS), which is a shape of a trajectory of center of pressure in the shank-fixed frame. Firstly, we show that ankle joints driven by flexible muscles antagonistically can generate a circular ROS by simple simulation and real robot experiments. Radius of the ROS can be controlled by tension of the muscles. Then, we demonstrate stable 3D limit cycle walking by a biped robot with flat feet using the proposed ROS controlling method. We also investigate its behavior and stability when extra load is added to the robot and verified that the stability of the robot is maintained by keeping the ROS. The results suggest that the ROS can be a stability measure for limit cycle walkers to realize adaptive walking.**

## I. Introduction

A passive dynamic walker can walk down on a gentle slope using gravitational energy [1]. This phenomenon suggests that high-performance electronic devices and complicated control programs may not be needed for biped robots' walking if their bodies are designed ingeniously. By adding small actuation to passive dynamic walkers, some researchers have developed so-called limit cycle walkers that can walk on a flat plane [2], [3], [4], [5], [6], [7]. Since these robots are well designed to utilize their body dynamics effectively, their walking is very energy efficient and the walking behaviors tend to be human-like, compared to the ZMP-based walking robots.

Most of limit cycle walkers have circular feet that give proper propulsion force to the robots. However, the circular feet confine robots' behavior only to walking. Their feet have to be replaced by flat feet or inverted arch feet in order to realize various behaviors such as standing, running, walking with various speeds, and so on. Although there have been some investigations about flat feet of limit cycle walkers [8], [9], the models of their simulation seems to be simplified excessively. For example, a collision between the foot and the ground is assumed to be completely inelastic since it is quite difficult to emulate the collision phenomenon accurately. It is also often assumed that the stance foot is always in contact with the ground horizontally in their virtual simulations, whereas there are at least three states in real situations; heel contact, toe contact, and full contact. Furthermore, most of simulation models are constrained to a sagittal plane, so more realistic theories are needed for a real biped robot that walks in a three-dimensional world.

On the other hand, some researchers of biomechanics have proposed that ROS (roll-over shape) can be a new paradigm for stable walking. ROS is defined as the shape of a series of COP (center of pressure) of a stance foot transformed into a shank-based coordinate system (ankle-knee coordinate system). Hansen et al. [10], [11] have indicated that the human ankle-foot system has a simple function during the period between heel contact and opposite heel contact of walking: to create an appropriate geometry, ROS. They analyzed human walking to figure out that the ROS maintains a similar circular shape under various conditions such as added weight, different heel height of shoes, and different walking speed. Meanwhile, a limit cycle walker with circular feet and rigid ankle joints also has a circular ROS since its stance foot touches the ground at one point in the sagittal plane and the shank-based coordinate system is determined uniquely by the contact point. Thus, circular feet of limit cycle walkers have the function to create a circular ROS, which leads to stable walking.

In this paper, we hypothesize that the ROS can be a useful indicator for controlling of the ankle joint of a limit cycle walker with flat feet. In other words, if ankle joints are controlled to generate a proper circular ROS, the robot with flat feet can walk as well as a robot with circular feet. We also hypothesize that the adaptability of the robot can be improved with the control of ankle joint to maintain a proper ROS. The robot with this control may be able to walk stably even when the body dynamics changes by adding extra load. In order to generate such a circular ROS, we focus on a human-like musculoskeletal structure. Instead of active and complicated control, we especially employ passive elastic elements to create a circular ROS automatically. Our goals are to realize 3D limit cycle walking of a real biped robot with flat feet by utilizing musculoskeletal structure and a simple limit cycle controller based on [7] and to verify two hypotheses mentioned above.

First, we explain the mechanism of generating a circular ROS with a musculoskeletal structure by using a quite simple ankle-foot model in section II. Second, we mention walking experiments of a humanoid robot with flat feet and musculoskeletal structure in section III. We examine its behavior and stability with various ankle stiffness, analyzing the ROS. We also investigate the change of the stability when extra load is added to the robot and propose the way to keep

This work was supported by Asada Synergistic Intelligence Project, ERATO, JST. All authors are with Dept. of Adaptive Machine Systems, Osaka Univ., 2-1 Yamadaoka, Suita, Osaka, 565-0871, Japan.
kenichi.narioka@ams.eng.osaka-u.ac.jp
shinpei.tsugawa@ams.eng.osaka-u.ac.jp
hosoda@ams.eng.osaka-u.ac.jp

the stability by utilizing the ROS. Finally, We conclude with the results and discuss future works in section IV.

## II. Simplest Ankle-Foot Model

First of all, we will explain how to calculate the ROS by using a simplest ankle-foot model. Then, we will mention a small experiment we did, which investigates the condition under which the ROS of the ankle-foot model becomes a circular shape.

### A. Method of Measuring ROS

A simple ankle-foot model is shown in Fig.1. This 2D model consists of a body, a leg, an ankle joint, and a flat foot, which contacts the ground at the heel and the toe. The body rolls over the ankle joint from left to right in the $x-z$ plane. $\sum$ represents the laboratory coordinate system, whose origin $O$ is fixed to the world and it is at the same position as the ankle joint in this simple model. Note that $O$ is not the same as the ankle position if the ankle is not fixed in more complicated and realistic model.

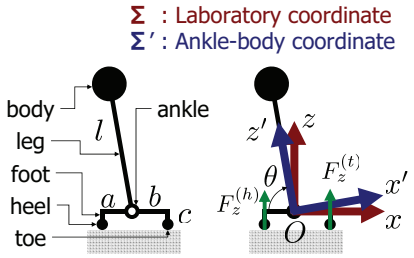


Fig. 1. Ankle-foot model

First, we have to measure a series of ground reaction forces at the toe ($F_z^{(t)}(t)$) and the heel ($F_z^{(h)}(t)$) in order to calculate COP as follows.

$$\begin{aligned} x(t) &= \frac{-aF_z^{(h)}(t) + bF_z^{(t)}(t)}{F_z^{(h)}(t) + F_z^{(t)}(t)} \\ z(t) &= -c \end{aligned} \tag{1}$$

Here, $x(t), z(t)$ are $x$-coordinate and $z$-coordinate of COP at time $t$, respectively. Next, a ROS is calculated by transforming COP into shank-based coordinate system $\sum'$ (represented by $x'$-axis and $z'$-axis), whose origin is always at the ankle joint and $z'$- coordinate is conformed to the leg (determined by $\theta(t)$).

$$\begin{aligned} x'(t) &= x(t)\sin\theta(t) + z(t)\cos\theta(t) \\ z'(t) &= -x(t)\cos\theta(t) + z(t)\sin\theta(t) \end{aligned} \tag{2}$$

Here, $x'(t)$,$z'(t)$ are x'-coordinate and z'-coordinate of COP at time $t$. Now we can get a ROS by plotting ($x'(t)$, $z'(t)$) over one walking cycle. Note that time $t$ should be from a heel strike to the next heel strike in a normal biped walking model. Since our single leg model has no 'next heel strike', we start to plot the data with an initial condition and stop to plot when $F_z^{(t)}(t)$ or $F_z^{(h)}(t)$ become negative.

### B. Effect of Compliant Ankle Joint

Human body parts are connected by compliant antagonistic muscles. We hypothesize that this musculoskeletal structure plays a great roll to generate a circular ROS. In order to prove this hypothesis, we did a small experiment with the ankle-foot model, adding virtual muscles to the ankle joint. We assumed that only the body had weight $m$ and the other parts had no weight. Then, equations of equilibrium of force, equilibrium of torque, and conservation law of energy are as follows.

$$\begin{aligned} (F_x^{(h)}(t) + F_x^{(t)}(t)) + F_l(t)\cos\theta(t) &= 0 \\ F_z^{(h)}(t) + F_z^{(t)}(t) &= F_l(t)\sin\theta(t) \\ c(F_x^{(h)} + F_x^{(t)}) + bF_z^{(t)} + \tau(t) &= aF_z^{(h)} \\ F_l(t) + \frac{mv(t)^2}{l} &= mg\sin\theta(t) \\ \frac{1}{2}mv(t)^2 + mgl\sin\theta(t) &= E_0 + \int \tau(t)\dot{\theta}(t)dt \end{aligned} \tag{3}$$

Here, $F_x^{(h)}(t), F_x^{(t)}(t)$ are friction forces from the ground to the heel and the toe, respectively. $F_l(t)$ is the force from the foot to the leg, $v(t)$ is the velocity of the body, and $E_0$ is initial mechanical energy.

We did numerical analyses of the simultaneous equations (3) with an initial condition and various input torques $\tau(t)$ in order to find out which type of $\tau(t)$ can generate a circular ROS. As a result, we found that the ROS become circular when $\tau(t) = k\cos\theta(t)(k = \text{const.})$, which confirms our hypothesis; compliance of the ankle joint can create a circular ROS. One typical result is shown in Fig.2 with the parameters set as shown in Table I. This graph shows that the ROS of the simplest ankle-foot model becomes circular shape.

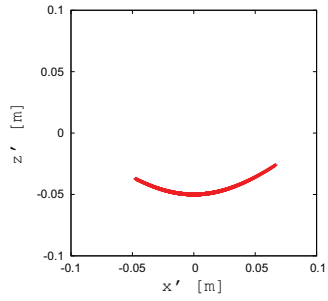


Fig. 2. ROS generated by compliant ankle

It seems desirable to implement the musculoskeletal structure as shown in Fig.3(a) in order to input the torque $\tau(t) = k\cos\theta(t)$ to a real robot, because we can easily change both angle and compliance of the ankle joint. On this account, we also measured the COP and the ROS with the musculoskeletal model, which has an antagonistic pair of spring. The result is shown in Fig.3(b). We have confirmed that the musculoskeletal structure plays a role to generate a circular ROS. This result is the groundwork of our hypothesis : if ankle joints are controlled to generate a circular ROS,

TABLE I
PARAMETERS OF NUMERICAL ANALYSIS

| Parameter | value |
|---|---|
| $k$ | 13 |
| $a$ | 30 mm |
| $b$ | 70 mm |
| $c$ | 50 mm |
| $l$ | 1000 mm |
| $m$ | 10 kg |
| $\theta(0)$ | 0.4 $\pi$ rad |
| $\dot{\theta}(0)$ | 0.3 $\pi$ rad |

the robot with flat feet can walk as well as the robot with circular feet.

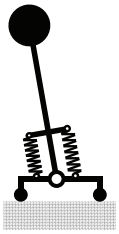

(a) Ankle-foot model with musculoskeletal structure

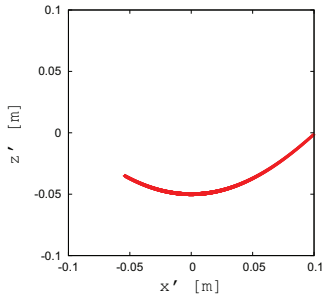


(b) ROS

Fig. 3. ROS generated by the musculoskeletal model

## III. 3D BIPEDAL WALKING OF REAL ROBOT

In this section, we address 3D biped walking of a real robot with flat feet. We measured the ROS by using pressure-sensitive sensors on the feet and a motion capture system. We examine its behavior and stability with various ankle stiffness, analyzing the ROS. We also investigate the change of the stability when extra load is added to the robot and propose the way to keep the stability by utilizing the ROS.

### A. Pneumat-BT with Flat Feet

Fig.4 shows the musculoskeletal humanoid robot named "Pneumat-BT". Thanks to new flat feet we built up, it can easily keep the standing posture, which is difficult for the robot with circular feet. Its height, width, leg length, thigh length, shank length and foot height are 1120 mm, 320 mm, 670 mm , 280 mm , 360 mm , and 50 mm, respectively. The robot is designed to be self-contained: it has all air valves, control boards, and a battery on the body. It also has FSR sensors on the four corners of each foot for two purpose: to detect heel contact and to measure the COP. We can put $CO_2$ cartridges for supplying air, but they are not actually used for the experiments in this paper because of the running costs. Instead, a compressor is used to supply 1 MPa compressed air to the regulator. The pressure to the air valves is regulated in 0.60 MPa. The robot weighs approximately 10.6 kg excluding the cartridges. Each joint of the robot is driven by an antagonistic pair of pneumatic actuators. We adopt McKibben pneumatic artificial muscles (shown in Fig.5) to drive the joints. Although the robot has 13 DOF, we actively drove only 4 DOF (hip joints and knee joints), while the other muscles are treated as adjustable compliant elements in the following experiments. In Fig.6(a), we show a sketch to describe how the joints are driven by pairs of pneumatic artificial muscles. The abbreviated names of the muscles are shown in Fig.6(b).

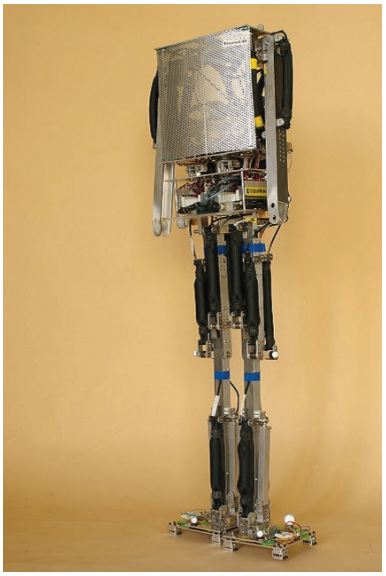

Fig. 4. Pneumat-BT with flat feet

Fig. 5. McKibben pneumatic artificial muscle : contraction as air supplied (above) and expansion as air exhausted (below)

### B. Walking Behavior

The robot is driven by a simple open-loop controller, which is basically same as our existing controller [7] as

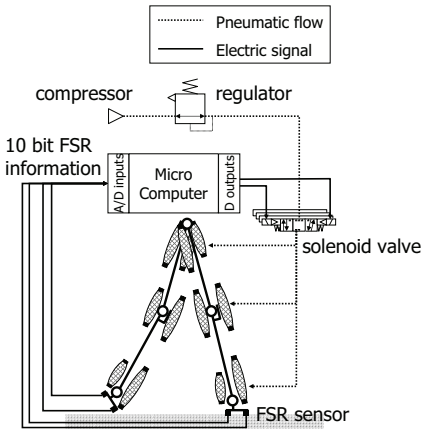


(a) Electronic and pneumatic system

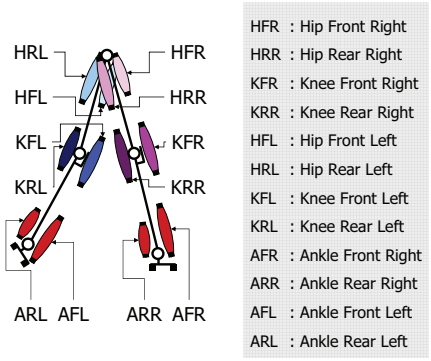


(b) Abbreviated name of muscles

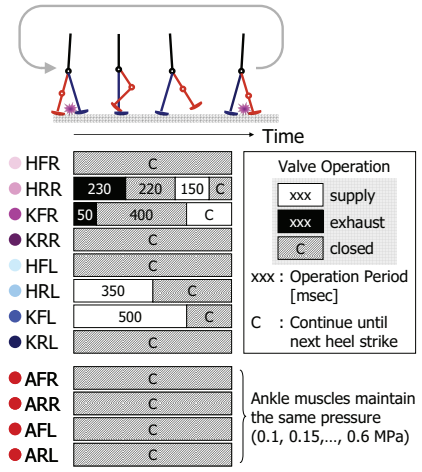


(c) Valve operation pattern

Fig. 6. Control architecture of Pneumat-BT

shown in Fig.6(c), in which the right leg is a swing leg at first. The controller gives a certain activation pattern to each muscle within one walking cycle, which is triggered by a heel strike. In this experiment, the valve operation patterns of muscles are as follows.

- A certain amount of air is given to the hip front muscles of both legs (HFR and HFL in the Fig.6(c)) only before a walking trial and kept that amount through the trial, while the air is exhausted from the hip rear muscle of swing leg (HRR) and supplied to the hip rear muscle of stance leg (HRL) in the early period of a walking cycle. These operations make the bending motion of the swing leg and stretching motion of the stance leg, respectively. They also supply the air to HRR in the latter period of the cycle, which make the retraction motion of the swing leg.
- The air is exhausted from both the knee front and rear muscles of the swing leg (KFR and KRR), which makes the knee joint free so that the knee bend naturally to pass the ground around midstance. After that, the air is supplied to KFR to stretch the knee.
- Muscles of the arms and the waist are constant around 0.60 MPa throughout one walking trial.
- Inner pressure of muscles of the ankles $P_a$ are constant around 0.10, 0.15, 0.20, 0.25, 0.30. 0.35, 0.40, 0.45, 0.50, 0.55, or 0.60 MPa throughout one walking trial.

In order to keep the balance in the frontal plane and the horizontal plane, the angle and stiffness of ankle roll joints are adjusted , which is the same method as [7].

### C. ROS Analysis

We calculated the COP from the data of the GRF on the four corners of each foot, using FSR sensors. We also measured the positions of the toe, heel, ankle, and knee of each leg, using a motion capture system VICON. Then, we calculated the ROS of the robot with various ankle stiffness and approximated it by an arc. As an example, the ROS and the approximated arc are shown in Fig.7 (when $P_a = 0.3$MPa). We ignored the ROS around heel in the approximation process. The ROS becomes circular in each case, while the curvature radius of the ROS varies according to the stiffness.

We also calculated the ROS of the robot with the load (1.06 kg, approximately 10% of the robot's mass), which is added to the hip and arms. Fig.8 shows the relationship between the curvature radius of the ROS, ankle stiffness, and the extra load. Note that we eliminated the data of the ROS which seems eccentric due to measurement errors and/or the inferior arc fitting algorithm. Dash lines are linear approximation of the curvature radius of the arc. The radius tends to be proportional to the ankle stiffness. It is also shown that the extra load reduces the gradient of the line. This graph means that we can operate the ROS by controlling the ankle stiffness.

We measured the walking stability of the robot by counting total walking steps of 20 walking trials with various ankle stiffness, as shown in Fig.9. The robot without load walked

130 steps until it felled down 20 times when $P_a = 0.3$MPa, which was most stable. On the other hand, the robot with load walked 102 steps through 20 trials when $P_a = 0.4$MPa, which was the best score with added load. Those walking behaviors are shown in Fig.11 and Fig.12, respectively.

Combining Fig.8 and Fig.9, we clarify the relationship between the ROS and walking stability as shown in Fig.10. The gap of two peaks of the stability seems to be smaller than that of Fig.9, which indicates that the ROS with which the robot can walk the most stably is constant even with the extra load.

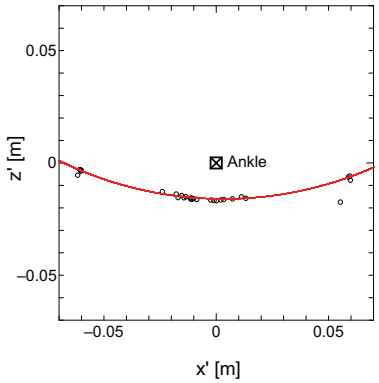


Fig. 7. ROS and approximated arc (Pa = 0.3 MPa)

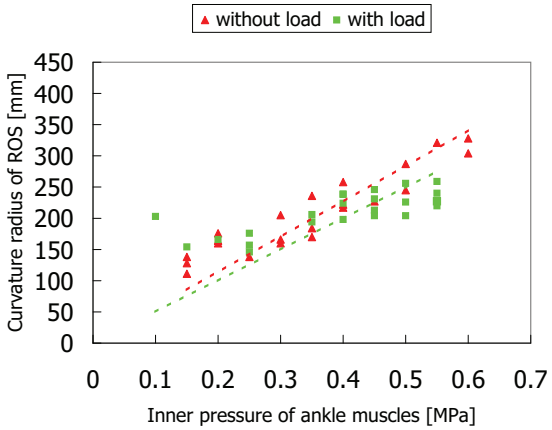


Fig. 8. Relationship between ankle stiffness and ROS

## IV. Conclusion and Discussion

In this paper, we have proposed the way to substitute the arc feet of traditional limit cycle walkers with the flat feet. Our key idea is that the shape of the arc feet corresponds to a circular ROS. First, we explained the mechanism of generating a circular ROS with musculoskeletal structure using the simple simulation model and the real biped robot. It is found that the curvature radius of the ROS can be controlled by the tension of the muscles. Then, we demonstrated stable 3D limit cycle walking by a biped robot with flat feet using the proposed ROS controlling method.

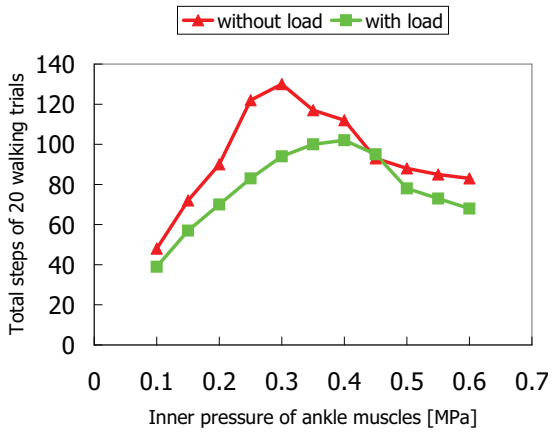


Fig. 9. Relationship between ankle stiffness and walking stability

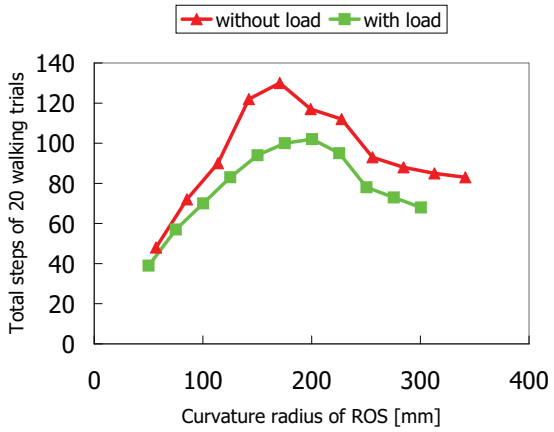


Fig. 10. Relationship between ROS and walking stability

We also tried to verify our advanced hypothesis : if an optimal curvature radius of the ROS is maintained by controlling ankle joints, the robot can walk stably even if the extra mass is loaded to the robot. This speculation is based on the result of the Hansen's work[10], [11]. In regard to this point, we compared the walking stability of the robot with load and without load. The result shows that the robot can walk most stably with the similar ROS in both cases, which can be a great support of the hypothesis.

A big issue is still remaining. We have not found how to maintain the ROS in real time as humans do. The fact that curvature radius of the ROS is proportional to the ankle stiffness can be useful for building a new control strategy. If the robot can maintain the ROS in various environments, the walking behavior of the robot can become quite adaptive.

## References

[1] T.McGeer. Passive dynamic walking. *Int. J. of Robotics Research*, Vol. 9, No. 2, pp. 62–82, 1990.

[2] M.Wisse and J. van Frankenhuyzen. Design and construction of mike; a 2D autonomous biped based on passive dynamic walking. *Proc. of the 2nd International Symposium on Adaptive Motion of Animals and Machines*, 2003.

Fig. 11. Walking behavior of Pneumat-BT without extra load (Pa = 0.30 MPa)

Fig. 12. Walking behavior of Pneumat-BT with extra load (Pa = 0.40 MPa)


[3] M.Wisse. Three additions to passive dynamic walking; actuation, an upper body, and 3D stability. *IEEE-RAS/RSJ International Conference on Humanoid Robots*, 2004.

[4] Steven H. Collins, and Andy Ruina. A bipedal walking robot with efficient and human-like gait. *Proc. of the 2005 IEEE Int. Conf. on Robotics and Automation*, pp. 1995–2000, 2005.

[5] Takashi TAKUMA, Koh HOSODA, and Minoru ASADA. Walking stabilization of biped with pneumatic actuators against terrain changes. *IEEE/RSJ International Conference on Intelligent Robots and Systems*, pp. 2775–2780, 2005.

[6] Koh Hosoda, Kenichi Narioka. Synergistic 3D Limit Cycle Walking of an Anthropomorphic Biped Robot. *IEEE/RSJ International Conference on Intelligent Robots and Systems*, pp. 470–475, 2007.

[7] Kenichi Narioka, Koh Hosoda. Designing Synergistic Walking of a Whole-Body Humanoid driven by Pneumatic Artificial Muscles: An empirical study. *Advanced Robotics*, Vol.22 No.10, pp.1107-1123,2008.

[8] M.Wisse, D. Hobbelen, R.Rotteveel, S.Anderson, and G.Zeglin. Ankle springs instead of arc-shaped feet for passive dynamic walkers. *IEEE-RAS/RSJ International Conference on Humanoid Robots*, 2006.

[9] Fumihiko Asano and Zhi-Wei Luo. On Energy-Efficient and High-Speed Dynamic Biped Locomotion with Semicircular Feet *IEEE/RSJ Int. Conf. on Intelligent Robots and Systems pp. 5901–5906*, 2006

[10] Hansen, Childress, Knox. Roll-over Shapes of Human Locomotor Systems: Effects of Walking Speed. Clinical Biomechanics, Vol. 19, No. 4, 407-414, 2004.

[11] Hansen, Childress. Effects of Shoe Heel Height on Biologic Roll-over Characteristics During Walking. Journal of Rehabilitation Research and Development, Vol.41, No.4, 547-554, 2004